Applied Chemical Engineering (2023) Volume 6 Issue 3
doi: 10.24294/ace.v6i3.2024

ORIGINAL RESEARCH ARTICLE

Phyto-fabrication of zinc oxide nanoparticles using *Ficus religiosa* and its potential application in degradation of crystal violet dye

Bhamini Pandey, Hema Tewatia, Dipendra Meel, Poonam Singh*

Department of Applied Chemistry, Delhi Technological University, Delhi 110042, India

*** Corresponding author:** Poonam Singh, poonam@dtu.ac.in

ABSTRACT

Herein zinc oxide (ZnO) nanoparticles have been synthesized via a facile, environment friendly, and low-cost green synthesis method. The prepared metal oxide was characterized using powder X-ray diffraction (PXRD), Fourier transform infrared spectroscopy (FTIR), SEM/EDX (scanning electron microscopy/energy dispersive X-ray), volumetric analysis, and zeta potential measurements. The photocatalyst was then employed for the degradation of crystal violet (CV) dye under UV illumination (high-pressure Hg lamp 125 W). It was observed that phyto-fabricated ZnO nanoparticles exhibited high degradation efficiency towards CV dye as 95% of dye was degraded in 60 min of irradiation. The study also implies that phyto-fabrication of ZnO nanoparticles resulted in enhanced degradation efficiency of the photocatalyst.

Keywords: crystal violet; photocatalysis; nanoparticles; zinc oxide; water treatment

ARTICLE INFO

Received: 12 April 2023
Accepted: 9 August 2023
Available online: 28 September 2023

1. Introduction

The availability of safe drinking water has become an alarming issue for the entire world in the last few decades due to rapid industrialization, urbanization, population growth, and climate change. Developing wastewater treatment technologies is an increasingly important global issue due to the limited availability of fresh and clean water[1]. A significant surface area-to-volume ratio, low production costs, and high stability make metal oxide-based nanomaterials ideal for water treatment[2].

Traditionally, nanomaterials can be synthesized via two synthetic approaches, i.e., bottom-up and top-down approaches as represented in **Figure 1**. The top-down synthesis techniques were used to produce micron-sized particles. However, the surface imperfections are one of the main drawbacks of constructing top molecules or clusters-by-clusters. On the other hand, the ‘bottom-up’ method generates less waste and is therefore more economical[3]. The process involves building molecules-by-molecules, atoms-by-atoms, or clusters-by-clusters where very small particles can be prepared and the possibility to control the size of particles. The conventional methods of synthesis of metal oxide nanoparticles (MONPs) are cost-ineffective, require the use of toxic precursors, and result in poor yield and aggregation of nanoparticles. Hydrolysis, precipitation, sol-gel, pyrolysis, solvothermal, and hydrothermal methods are some of the chemical techniques that have been used for the preparation of

MONPs, but they always involve usage of toxic reagents, lengthy processes, and an environmental waste generation problem[4]. The conventionally synthesized nanoparticles have been found to be toxic, so are also not suitable for clinical use.

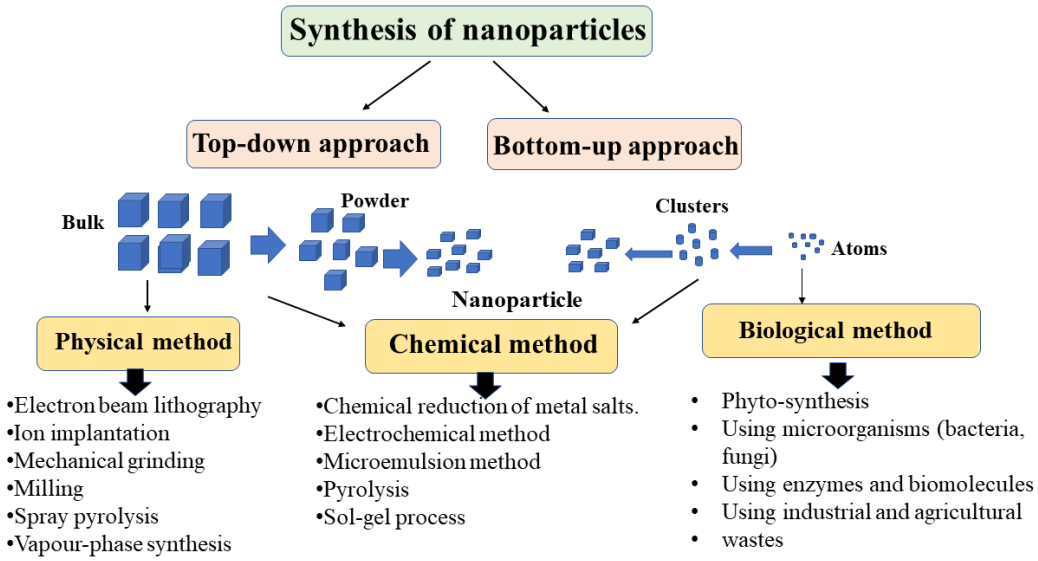

Figure 1. Different approaches to synthesize metal oxide nanoparticles (MONPs).

To overcome the drawbacks of traditional synthesis approaches, plant extract-mediated synthesis of MONPs has been adopted in recent years based on the principles of green chemistry[5]. Green synthesis approaches have gained attention due to their ability to avoid use of toxic chemicals, high costs, and harsh conditions during the stabilization and reduction processes. In order to control the growth of crystals, plant, fruit, and vegetable extracts are used as stabilizers and reducing agents[6]. In the process of making metal oxide nanoparticles, plants utilize secondary metabolites, proteins, enzymes, and other reducing agents. The *Ficus religiosa* tree, also known as the peepal tree in India, Pakistan, and Bangladesh, is holy[7]. In the traditional system, leaves, roots, fruit, and bark of peepal tree were used in pharmaceuticals[8]. The leaves of *Ficus religiosa* contain several phytochemicals such as myricetin, kaempeferol, vitamin-K, n-octacosanol, and quercetin, which act as stabilizing as well as a reducing agent that can be used to cap and protect metal oxide nanoparticles during their synthesis. These metal oxide nanoparticles can be used efficiently for the removal of toxic effluents from synthetic and real water samples via various approaches such as adsorption, membrane filtration, photocatalysis, etc. Among all the reported methods the photocatalytic degradation of effluents exhibits several advantages, such as no toxic by-products, energy efficiency, economic viability, etc.

Titanium dioxide (TiO_2), zinc oxide (ZnO), copper oxide (CuO), and other transition metal oxides may be considered outstanding semiconducting materials that can disintegrate organic pollutants such as dyes from polluted water by absorbing light photons[9]. In recent years, it has been found that ZnO nanoparticles can be easily tuned by changing their morphology, resulting in unique optical and chemical properties. In the biomedical field, in the rubber industry, and for metal surface treatment, zinc oxide has many unique properties that make it of economic and industrial importance. There are many active sites in the semiconductor photocatalyst ZnO[10]. It also shows remarkable optical and photocatalytic properties due to its similar band gap to TiO_2 (3.2 eV for anatase)[11]. Surface-to-volume ratios of ZnO nanoparticles are high and they have 3.3 eV broad bandgaps and 60 MeV binding energies. A key reason for ZnO's impressive photocatalytic properties is its exciting chemical and physical stability, superoxidative capability, and low toxicity. The recombination of holes and electrons is prevented by defects on the surface and in the core, such as zinc, oxygen interstitials, and oxygen vacancies. As a result, superoxide and hydroxyl radicals are

produced, which contribute to dye degradation through photocatalysis. The textile industry has extensively utilized cationic azo dyes such as crystal violet for several years. In recent years, various metal oxide nanoparticle-based photocatalysts have been studied for the photocatalytic degradation of CV dye. A study by Saini et al. used *Azadirachta indica* bark and seed extract to synthesize ZnO nanoparticles and studied its photocatalytic activity toward methyl orange dye. It was reported that 84.62% of dye was degraded in 180 min of light irradiation[12].

In the present study, aqueous *Ficus religiosa* leaf extract and zinc acetate were used as precursors to synthesize zinc oxide nanoparticles (ZNPs). PXRD, FTIR, SEM/EDX, complexometric estimation, and zeta potential analysis were used to confirm the structural properties of synthesized ZNPs. Photocatalytic degradation of crystal violet dye from contaminated water was accomplished with the synthesized zinc oxide nanoparticles. An effective dye degradation rate of 95% was achieved within 60 min at a 10 ppm concentration of CV dye solution. The phytochemically synthesized zinc oxide acts as a more efficient catalyst for photodegradation of CV dye in comparison to zinc oxide nanoparticles synthesized without using plant extract.

2. Experimental procedure

2.1. Collection of plant materials

The leaves of *Ficus religiosa* used for synthesis of nanoparticles were collected from the science block of Delhi Technological University, Delhi, India.

2.2. Preparation of leaf extract from *Ficus religiosa*

In order to make a fine powder of *Ficus religiosa* leaves, the leaves were first carefully cleaned with deionized (DI) water, then shade-dried and ground to make a fine powder. 50 g of the powdered leaves were then added to 500 mL of distilled water and kept for 72 h at room temperature. Afterward, the solution was filtered and the plant extract was stored at a low temperature.

2.3. Preparation of zinc oxide nanoparticles using *Ficus religiosa* leaf extract

For synthesis of ZnO nanoparticles, first to 10 mL of zinc acetate solution (1 M), 30 mL of leaf extract (1:3) was added dropwise. The solution was then kept on stirring for 10 min and pH 11 of the solution was maintained using NaOH. The resultant mixture was stirred further for 30 min and sonicated for an hour followed by stirring with heating at 60 ℃ for 30 min. Finally, the product obtained was filtered and oven-dried.

Calcination*:* The yellow-colored powder obtained was further collected in a quartz crucible and sintered at 350 ℃ in a muffle furnace for 3 h to obtain zinc oxide nanoparticles (ZNP1).

Similarly, zinc oxide nanoparticles were synthesized without using plant extract and labeled as ZNP2. The schematic representation of synthesis of ZnO nanoparticles with and without *Ficus religiosa* leaf extract is depicted in **Figure 2a,b**, respectively. In addition, the possible mechanism of green synthesis of ZNP1 is presented in **Figure 3**.

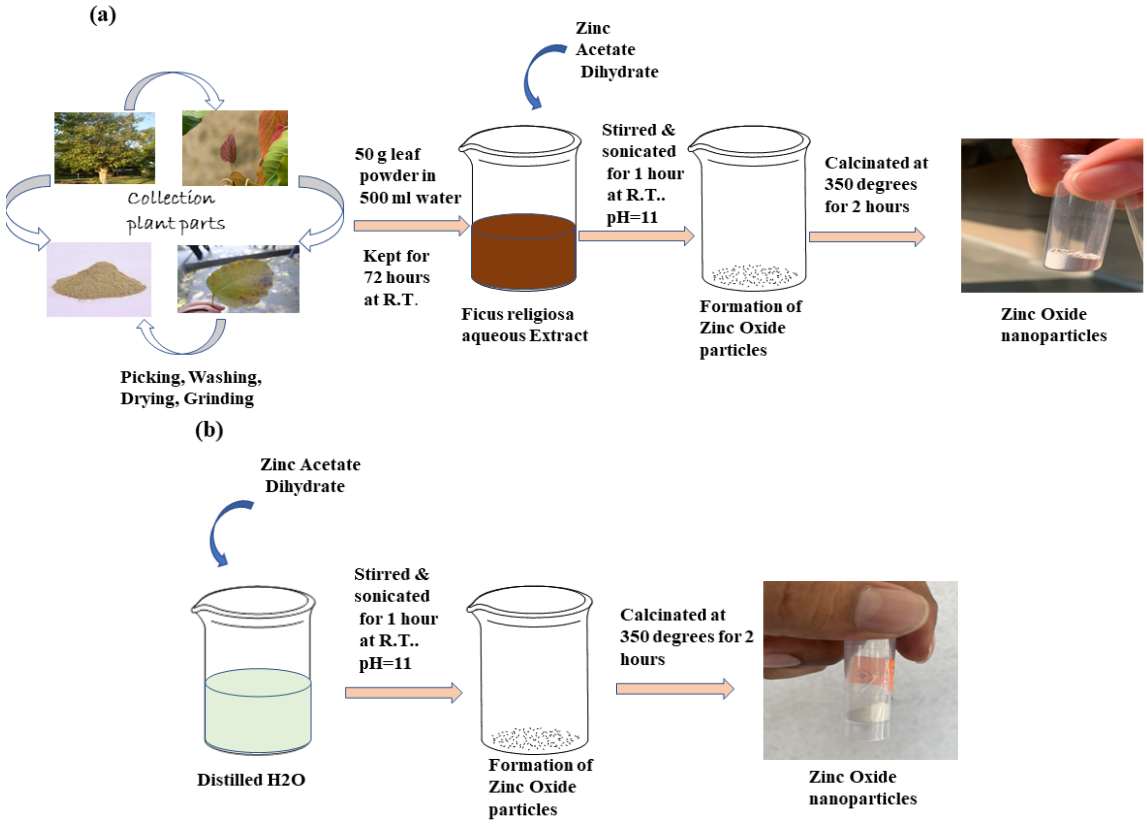

Figure 2. Synthesis of zinc oxide nanoparticles **(a)** using leaf extract of *Ficus religiosa*; and **(b)** without plant extract.

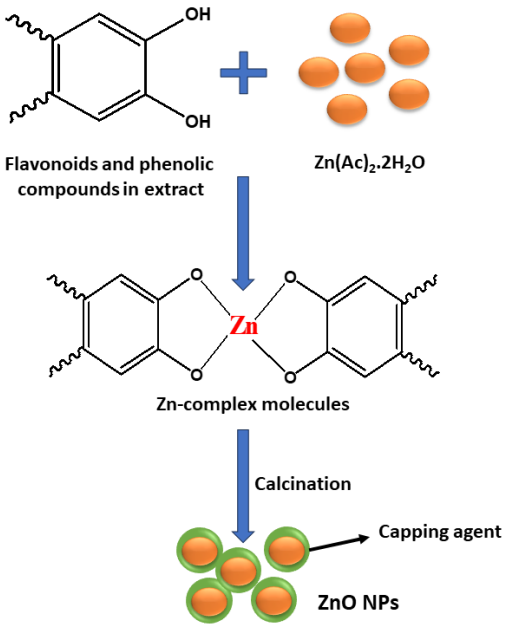

Figure 3. Plausible mechanism of ZnO nanoparticles synthesis using *Ficus religiosa* leaf extract.

2.4. Characterization

The PXRD pattern of ZnO was recorded using Bruker D8 diffractometer with 0.02 step size in the 2θ range of 5°–70°. The chemical composition of the synthesized ZnO was examined by FTIR-ATR Perkin Elmer Frontier (50 Build-in Diamond ATR module). SEM with EDX analysis was performed using a Zeiss Gemini SEM. Pananalytic Zetasizer version 7.13 was used for zeta potential measurements.

2.5. Evaluation of photocatalytic activity

An annular horizontal cylinder batch reactor was used to photocatalyze crystal violet dye**.** The reactor was illuminated with a high-pressure mercury fluorescent lamp of 125 W. In the presence of a light source, crystal violet (CV) dye solution was photodegraded by ZnO to determine its photocatalytic activity. During the experiment, CV was dissolved in distilled water to prepare a stock solution. A 30 min magnetic stir before irradiation was done in order to achieve adsorption-desorption equilibrium between pollutant and photocatalyst. After that an exposure of light source was made to the dye solution in the presence of photocatalyst under constant stirring and 3 mL samples were withdrawn after a fixed interval of time and centrifuged for 5 min. The concentration of each was determined by using a carry 300 UV-vis spectrophotometer at λ_{max} value of 588 nm. The degradation percentage (%) was calculated using Equation (1) after degradation in a wavelength range of 200 to 800 nm.

$$\%\, Degradation = \frac{C_o - C}{C_o} \times 100 \quad (1)$$

where C is the concentration of the CV dye solution in reaction mixture with photocatalysts after light irradiation for time t and C_0 denoted the initial concentration of CV without catalysts. Beer-Lambert's law was used to establish a calibration plot that relates absorbance to concentration to determine the unknown concentration of dye.

3. Result and discussion

3.1. Characterization of photocatalyst

The X-ray diffraction (XRD) results of phyto-fabricated metal oxide (ZnO) are shown in **Figure 4a** where broad reflections at 2θ values of 31.66, 34.35, and 36.15 correspond to hexagonal $P6_3mc$ space group. The reflection planes can be assigned the hkl values as (100), (002), and (101)[13]. The crystallite size of synthesized zinc oxide nanoparticles was calculated using the Debye-Scherer formula given in Equation (2).

$$D = 0.94\, \lambda/\beta\, \mathrm{Cos}\, \theta \quad (2)$$

where the average crystallinity is D, the wavelength is in $Å$, FWHM is β (in radian) and θ indicates the degree of diffraction. Based on the Scherrer equation the average size of the ZNP1 and ZNP2 was calculated to be 20.28 and 29.12 nm, respectively.

FTIR spectrum of phyto-nanofabricated zinc oxide nanoparticles was recorded in 4000–400 cm^{-1} range and is given in **Figure 4b**. The broad absorption band at 3360 cm^{-1} corresponds to the stretching vibration of O–H groups of water present as moisture. The bands at 876 and 844 cm^{-1} can be attributed to the Zn–OH stretching vibrations. The presence of metal-oxygen linkages (M–O) in the synthesized nanoparticles can be confirmed by the presence of bands in the range of 400–600 cm^{-1}. However, the additional bands present at 1550 and 1432 cm^{-1} can be ascribed to the presence of carbonyl groups of phytochemicals attached to ZNPs[12]. These findings suggest that the bio-synthesized ZnO NPs are capped by phytochemicals present in the leaf extract having various functional groups. Moreover, it can also be anticipated that the organic contents or phytochemicals present in the plant extract are responsible for the reduction and stabilization of synthesized ZNPs[14,15].

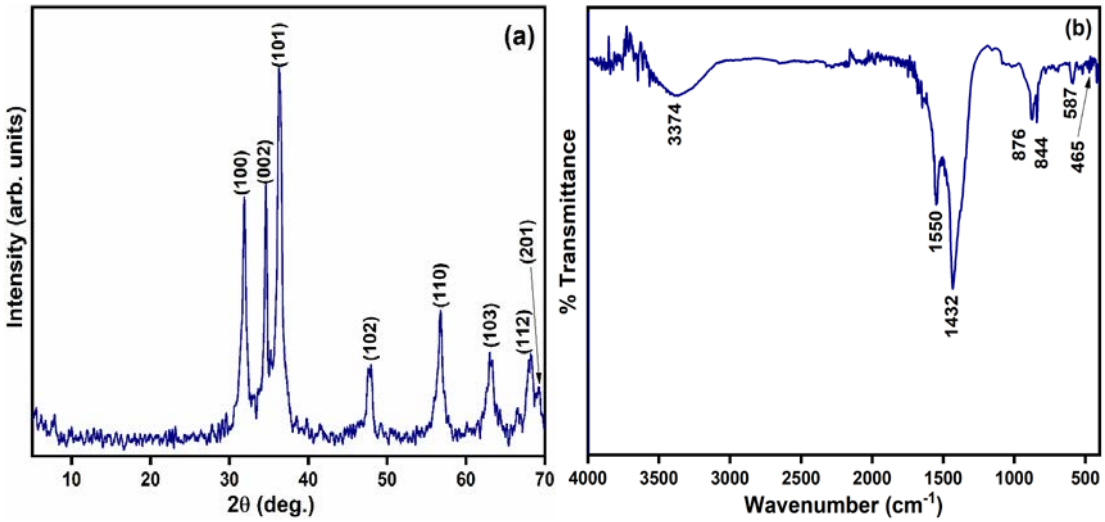

Figure 4. (a) PXRD pattern; and **(b)** FTIR spectrum of phyto-fabricated ZnO nanoparticles (ZNP1).

The SEM/EDX analysis was employed to examine the morphology, structure, and composition of zinc oxide NPs. From the SEM micrograph, it can be deduced that ZnO NPs are less agglomerated owing to the presence of leaf extract acting as a capping agent. **Figure 5a** shows EDX results confirming the presence of zinc nanoparticles in oxide form, which indicates that phyto-synthesis can be successfully employed to synthesize ZnO NPs. The SEM/EDX analysis of ZnO NPs before and after photodegradation was also carried out (**Figure 5a,b**). It was evident from the SEM images that the photocatalyst remains stable since no significant difference in the shape and morphology of catalyst was observed before (ZNP1) and after photodegradation suggesting its reuse as a catalyst for dye degradation. The elemental composition of NPs before and after photocatalysis is also presented in **Table 1** showing no significant change.

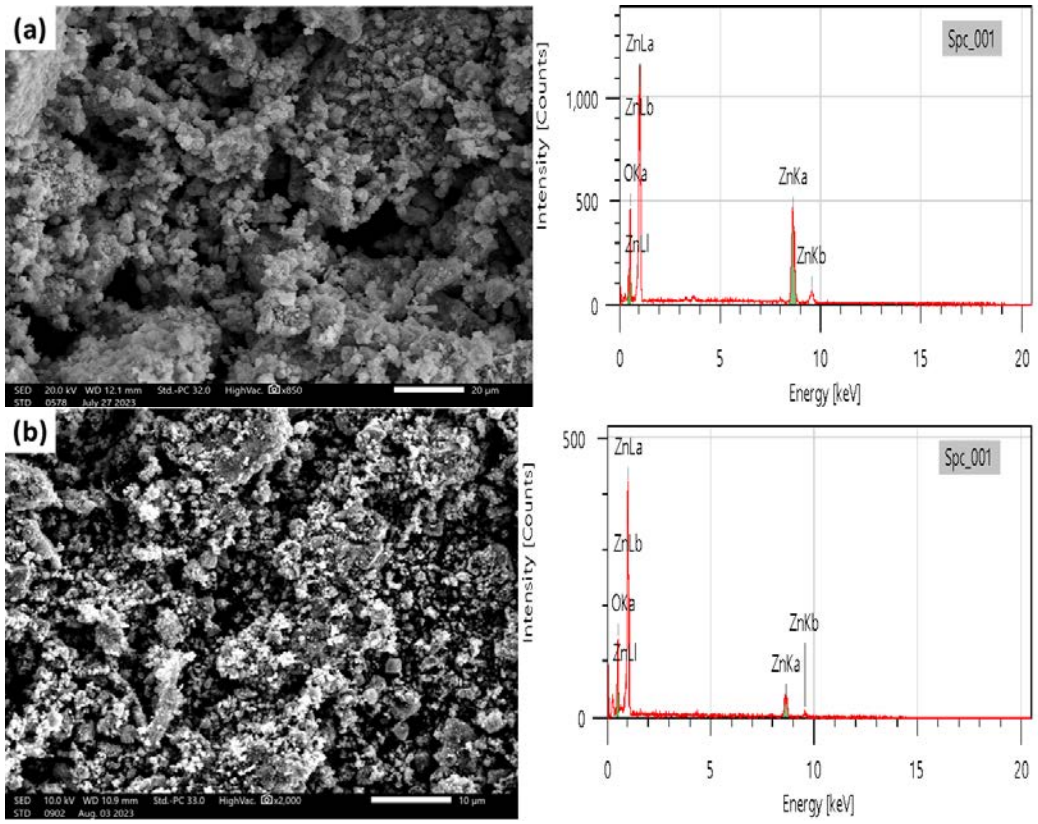

Figure 5. SEM/EDX images of ZNPs **(a)** before; and **(b)** after photodegradation.

Table 1. Elemental composition of ZnO NPs from EDX data.

	Elemental composition (%)	
Elements	**Before photodegradation**	**After photodegradation**
Zinc	82.76	81.35
Oxygen	17.24	18.65

The surface charge of synthesized nanoparticles was also estimated using zeta potential analysis and was found to be −26.4 mV indicating that the surface of ZNP1 is negatively charged. The negative zeta potential indicates the presence of negatively charged ions or functional groups on the surface of zinc oxide nanoparticles. These charged entities create an electrostatic repulsion among the nanoparticles, preventing their agglomeration or aggregation. The higher the negative zeta potential value, the stronger the repulsion and greater the stability of the nanoparticles in the solution.

The estimation of zinc ions in the synthesized lattice can provide detailed insights into the elemental composition of the synthesized nanoparticles. Therefore, volumetric analysis was carried out to determine the concentration of zinc ions in synthesized ZnO nanoparticles using complexometric titration. Standardized ethylenediamine tetraacetic acid (EDTA), ammonia buffer, and eriochrome black T (EBT) were used to determine the concentration of Zn metal ions, where EDTA and EBT were used as a complexing agent and indicator while ammonia buffer was added to maintain the pH of the solution, i.e., 10 pH. The % of zinc in the metal oxide nanoparticles was found to be 68%.

3.2. Photocatalytic studies

In this study, ZnO was used as a photocatalyst to degrade crystal violet under the influence of different variables including contact time, pH, catalyst dosage, and initial concentration of dye, in order to develop an integrated model for crystal violet degradation by photocatalysis.

3.2.1. Impact of irradiation time and plant extract on degradation of CV dye

In order to study the impact of irradiation time of photodegradation of dye, 0.05 g of photocatalyst (ZNP1) was added to 100 mL of 10 mg/L solution of CV dye. The spectral changes observed during the degradation of CV dye are presented in **Figure 6a** where it can be observed that 37% of dye was removed during adsorption process and degradation efficiency enhanced up to 95% within 60 min of irradiation time.

Later, the photocatalytic ability of ZnO nanoparticles without (ZNP2) plant extract was also carried out to compare the degradation efficiency. It was observed that within 60 min of irradiation time and similar reaction conditions, ZNP2 degraded only 80% of CV dye. The results obtained are given in **Figure 6b** which indicates that the phyto-fabricated ZnO NPs exhibited superior photocatalytic properties as compared to the metal oxide prepared without using leaf extract.

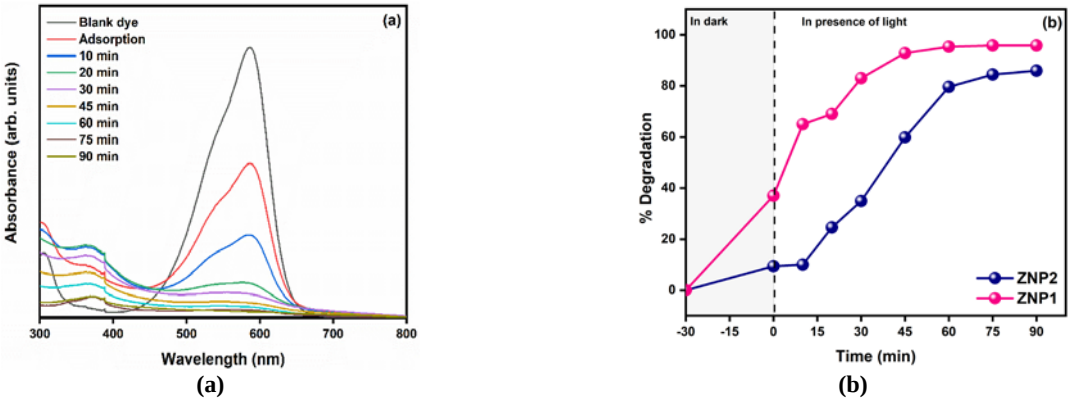

(a) **(b)**

Figure 6. Plot of **(a)** absorbance vs wavelength; and **(b)** rate of degradation vs irradiation time for photodegradation of CV dye.

3.2.2. Impact of pH of the solution

In the photocatalytic study, pH is an important operational variable, as it is responsible for the degradation of various dyes and other organic pollutants. Additionally, it played a significant role in practical wastewater treatment. From **Figure 7a** it can be deduced that low pH value (pH = 3) resulted in less than 70% photodegradation efficiency, however, on increasing the pH value of dye solution from 3 to 7, the photodegradation efficiency increased from 64.9% to 97%, respectively. These results indicated that at neutral pH conditions, there occurs an increase in number of hydroxyl radicals which leads to the enhanced photodegradation of CV dye.

3.2.3. Impact of initial dye concentration

In this experiment, 100 mL of dye solution was mixed with 0.05 g of catalyst having variable dye concentrations, i.e., 10, 20, and 60 mg/L under UV light irradiation, and the results obtained are presented in **Figure 7b**. The crystal violet dye degradation efficiency is inversely proportional to the dye concentration, so higher dye concentrations result in lower photodegradation efficiency. There occurs a decrease in degradation efficiency when the initial dye concentration increases from 10–60 mg/L. When the dye concentration is low, the available hydroxyl radicals (OH•) generated by the photocatalyst effectively interact with and degrade the dye molecules. However, as the dye concentration increases, a larger number of dye molecules compete for the available hydroxyl radicals. In essence, the hydroxyl radicals are being "consumed" by the dye molecules instead of efficiently degrading them.

3.2.4. Impact of dosage variation

In 100 mL of 10 mg/L dye solution, the amount of catalyst was varied from 0.025 g to 0.1 g to examine the efficacy of photodegradation of crystal violet with different catalyst loading doses. It is evident from **Figure 7c** that there has been an increase in photodegradation efficiency of photocatalysts from 65% to 97%. As a result of increased catalyst loading, the catalyst surface exhibits more active sites, which subsequently generate more holes and hydroxyl radicals. Thus, resulting in increased photodegradation efficiency of the NPs.

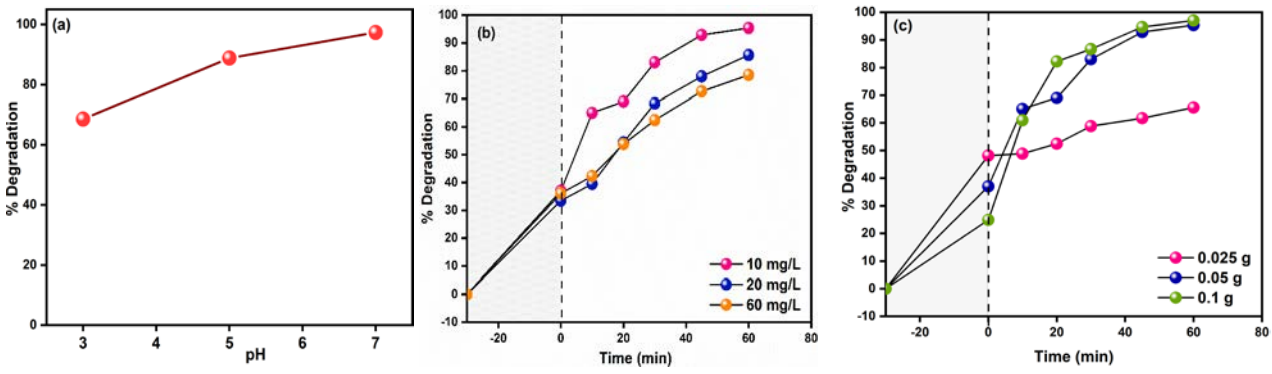

(a) **(b)** **(c)**

Figure 7. Plot of effect of **(a)** pH; **(b)** concentration of dye; and **(c)** amount of photocatalyst on % degradation of dye.

3.2.5. Degradation mechanism

By irradiating ZnO with light, electrons were excited from its valence band into the conduction band, resulting in electron-hole pair formation. Photocatalytic degradation occurs when electrons and holes are generated by oxidation, it releases highly reactive radical species, such as superoxide and hydroxyl radicals for non-hazardous degradation of dye molecules. As the electrons in the conduction band react with atmospheric oxygen, they form superoxide radical anions (**Figure 8**). As a result of the reaction between crystal violet dye and the superoxide radical anion, a variety of degradation products are produced[16]. The

photodegradation of CV dye occurs as follows:

$$\text{Zinc oxide} + h\nu \longrightarrow \text{Zinc oxide } (h^{+}_{VB} + e^{-}_{CB})$$

$$O_2 + e^- \longrightarrow O_2^{\bullet -}$$

$$CV + O_2^{\bullet -} \longrightarrow \text{Degraded products of CV}$$

$$H_2O + h^{+}_{VB} \longrightarrow OH^{\bullet} + H^{+}$$

$$CV + HO^{\bullet} \longrightarrow \text{Degraded products of CV}$$

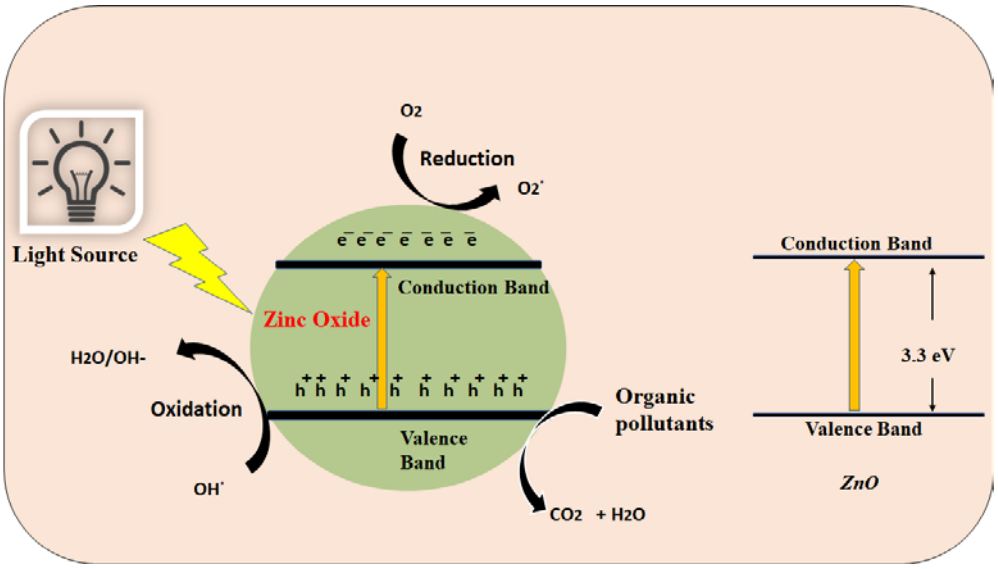

Figure 8. Mechanism of photocatalytic degradation.

3.2.6. Comparison with other ZnO-based photocatalysts

A comparison between some of the ZnO-based photocatalysts reported in the literature for the degradation of CV dye is presented in **Table 2**. The results indicate that the photocatalyst used in the present work showed high degradation efficiency within a short period of UV light irradiation. Additionally, no toxic precursors or extreme reaction conditions were employed for the synthesis of ZnO NPs in the present study. Therefore, the synthesized material could be considered as an efficient photocatalyst for CV dye degradation.

Table 2. Comparison of degradation efficiencies of different ZnO-based photocatalysts for CV dye degradation.

ZnO-based photocatalysts	Method of synthesis	Degradation efficiency (%)	Time (min)	Light source	References
ZnO nanonails ZnO nanorods	Thermal evaporation method	~95 82	70 70	UV	[17]
ZnO thin film	Spray pyrolysis technique	86	210	UV	[18]
ZnO-flowers	Precipitation method	~96	80	UV	[19]
ZnO	Precipitation method	88.84	24 h	UV	[20]
ZnO nanoparticles	Plant extract-mediated synthesis	86	90	Visible	[21]
ZnO nanoparticles	Plant extract-mediated synthesis	95	60	UV	Present study

3.2.7. Reusability of synthesized photocatalyst

One of the key factors of photocatalytic reactions is the recyclability of the catalyst, which represents the stability and activity of the catalyst. The reusability profile of photocatalyst is shown in **Figure 9**. The photocatalyst was washed with water and dried in oven then later used for the next photocatalytic cycle. It can be observed that the catalytic performance of the material decreased from 95% to 86% after 4th

regeneration cycle. Thus, suggesting that the material can act as an efficient catalyst for degradation of CV dye up to four cycles.

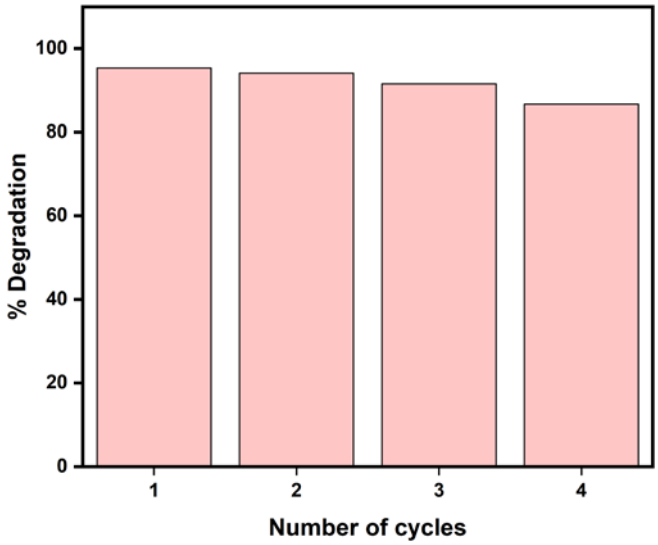

Figure 9. Reusability profile of ZnO nanoparticles.

4. Conclusion

In this study, a green, eco-friendly, and cost-effective approach was used to synthesize ZnO nanoparticles using leaf extract of *Ficus religiosa*. XRD, FTIR, SEM/EDX techniques as well as zeta potential measurements were used to characterize the synthesized sample. The percentage of metal content in the synthesized lattice was estimated using complexometric titration. Under light illumination, the photocatalytic performance of newly designed nanoparticles on CV dye degradation was investigated showing degradation of 95% of dye within 60 min of illumination. The catalytic efficiency of ZnO was found to be dependent on several factors, i.e., pH of dye solution, catalyst dosage, and initial dye concentration.

Author contributions

Conceptualization, BP and PS; methodology, BP and PS, software, BP, HT and DM; validation, BP and PS; formal analysis, HT and DM; investigation, HT and DM; resources, PS; data curation, HT and DM; writing—original draft preparation, HT and DM; writing—review and editing, BP and PS; visualization, BP and PS; supervision, PS; project administration, BP and PS. All authors have read and agreed to the published version of the manuscript.

Acknowledgments

The authors are grateful to the Delhi Technological University, DTU, India for providing the necessary facilities and support for this work. Author BP would also like to thank CSIR, India for providing financial assistance (SRF).

Conflict of interest

The authors declare no conflict of interest.

References

1. Pandey B, Singh P, Kumar V. Photocatalytic-sorption processes for the removal of pollutants from wastewater using polymer metal oxide nanocomposites and associated environmental risks. *Environmental Nanotechnology,*

Monitoring & Management 2021; 16: 100596. doi: 10.1016/j.enmm.2021.100596
2. Bandeira M, Giovanela M, Roesch-ely M, et al. Green synthesis of zinc oxide nanoparticles: A review of the synthesis methodology and mechanism of formation. *Sustainable Chemistry and Pharmacy* 2020; 15: 100223. doi: 10.1016/j.scp.2020.100223
3. Agarwal H, Kumar SV, Rajeshkumar S. A review on green synthesis of zinc oxide nanoparticles—An eco-friendly approach. *Resource-Efficient Technologies* 2017; 3(4): 406–413. doi: 10.1016/j.reffit.2017.03.002
4. Nava OJ, Soto-Robles CA, Gómez-Gutiérrez CM, et al. Fruit peel extract mediated green synthesis of zinc oxide nanoparticles. *Journal of Molecular Structure* 2017; 1147: 1–6. doi: 10.1016/j.molstruc.2017.06.078
5. Chavali MS, Nikolova MP, Silver A. Metal oxide nanoparticles and their applications in nanotechnology. *SN Applied Sciences* 2019; 1(6): 1–30. doi: 10.1007/s42452-019-0592-3
6. Bala N, Saha S, Chakraborty M, et al. Green synthesis of zinc oxide nanoparticles using *Hibiscus subdariffa* leaf extract: Effect of temperature on synthesis, anti-bacterial activity and anti-diabetic activity. *RSC Advances* 2015; 5(7): 4993–5003. doi: 10.1039/c4ra12784f
7. Bukhari SA, Ayub I, Iqbal A, Hussain MM. Green matrix based synthesis and characterization of nanoparticles of *Ficus religiosa* plant. *Asian Journal of Emerging Sesearch* 2020; 2(4): 188–189. doi: 10.3923/AJERPK.2020.188.189
8. Riyas ZM, Gayathri R, Prabhu MR, et al. Green synthesis and biomedical behavior of Mg-doped ZnO nanoparticle using leaf extract of *Ficus religiosa*. *Ceramics International* 2022; 48(17): 24619–24628. doi: 10.1016/j.ceramint.2022.05.107
9. Meena PL, Poswal K, Surela AK, Saini J. Facile synthesis of ZnO/CuO/Ag_2O ternary metal oxide nanocomposite for effective photodegradation of organic water pollutants. *Water Science and Technology* 2021; 84(9): 2615–2634. doi: 10.2166/wst.2021.431
10. Thattil PP, Rose AL. Enhanced removal of crystal violet dye using zinc oxide nanorods and air oxidation under sunlight radiation. *Rasayan Journal of Chemistry* 2020; 13(2): 1166–1173. doi: 10.31788/RJC.2020.1325558
11. An VN, Van TTT, Nhan HTC, Hieu LV. Investigating methylene blue adsorption and photocatalytic activity of ZnO. *Journal of Nanoparticles* 2020; 2020: 6185976. doi: 10.1155/2020/6185976
12. Saini M, Yadav S, Rani N, et al. Biosynthesized zinc oxide nanoparticles using seed and bark extract of *Azadirachta indica* for antibacterial, photocatalytic and supercapacitor applications. *Material Science and Engineering: B* 2022; 282: 115789. doi: 10.1016/j.mseb.2022.115789
13. Anil K, Vinod I, Shrivastava S. Photocatalytic degradation of methylene blue using ZnO and 2% Fe-ZnO semiconductor nanomaterials synthesized by sol-gel method: A comparative study. *SN Applied Sciences* 2019; 1(10): 1–11. doi: 10.1007/s42452-019-1279-5
14. Khalafi T, Buazar F, Ghanemi K. Phycosynthesis and enhanced photocatalytic activity of zinc oxide nanoparticles toward organosulfur pollutants. *Scientific Reports* 2019; 9(1): 6866. doi: 10.1038/s41598-019-43368-3
15. Khan SA, Shahid S, Shadid B, et al. Green synthesis of MnO nanoparticles using abutilon indicum leaf extract for biological, photocatalytic, and adsorption activities. *Biomolecules* 2020; 10(5): 785. doi: 10.3390/biom10050785
16. Kanagamani K, Muthukrishnan P, Saravanakumar K, et al. Photocatalytic degradation of environmental perilous gentian violet dye using leucaena-mediated zinc oxide nanoparticle and its anticancer activity. *Rare Metals* 2019; 38(4): 277–286. doi: 10.1007/s12598-018-1189-5
17. Tripathy N, Ahmad R, Song JE, et al. ZnO nanonails for photocatalytic degradation of crystal violet dye under UV irradiation. *AIMS Materials Science* 2017; 4(1): 267–276. doi: 10.3934/matersci.2017.1.267
18. Ameur SB, BelHadjltaief H, Duponchel B, et al. Enhanced photocatalytic activity against crystal violet dye of Co and in doped ZnO thin films grown on PEI flexible substrate under UV and sunlight irradiations. *Heliyon* 2019; 5(6): e01912. doi: 10.1016/j.heliyon.2019.e01912
19. Ameen S, Akhtar MS, Naim M, Shin HS. Rapid photocatalytic degradation of crystal violet dye over ZnO flower nanomaterials. *Materials Letters* 2013; 96: 228–232. doi: 10.1016/j.matlet.2013.01.034
20. Kathiresan G, Vijayakumar K, Sundarrajan AP, et al. Photocatalytic degradation efficiency of ZnO, GO and PVA nanoadsorbents for crystal violet, methylene blue and trypan blue dyes. *Optik* 2021; 238: 166671. doi: 10.1016/j.ijleo.2021.166671
21. Karthik P, Ravichandran S, Mukkannan A, Rajesh J. Plant-mediated biosynthesis of zinc oxide nanoparticles from *Delonix Elata*: A promising photocatalyst for crystal violet degradation. *Inorganic Chemistry Communications* 2022; 146: 110122. doi: 10.1016/j.inoche.2022.110122